Finite Element Analytical Techniques and Applications to Structural Design

Tawfik Khalil and Paul Du Bois

Analytical simulation of vehicle crashworthiness has evolved over the past 30 years. Three types of models are used to simulate vehicle structures - Lumped Parameter (LP) models, hybrid models, and Finite Element (FE) models. The FE models can be divided into two groups: heuristic beam models and continuum mechanics-based models which use beam, solid and shell elements. The progression of these models over the years followed a pattern of increasing geometric details since it was realized that a simple analytical model of the crash event, developed and tuned to fit one or more parameters from a specific test, does not ensure accurate prediction for all impact conditions. In fact, the most detailed models (LP or FE) developed to date should be considered approximations of a highly complex non-linear system that is often subject to large and unstable elastic-plastic deformations. Obviously, advances in understanding complex system performance such as crashworthiness can be achieved by increasingly including more details that capture realistic vehicle kinematics and loads encountered in general crash conditions.

This chapter provides an overview of the FE techniques used in vehicle body structural development to satisfy the design constraints necessary for the vehicle to meet myriad safety requirements expected of the vehicle structure and to assure vehicle crashworthiness. The analytical tools used to assess occupant response in crash and human tolerance to impact is addressed in another chapter. For completeness, recent models that integrate the occupant, restraint systems, and vehicle structure in a single analysis will be discussed in this chapter.

3.1 Historical Background

The history of structural crashworthiness analysis can best be characterized by two periods of historical development: an early period, extending from 1970 to

about 1985; and a second period beginning in the mid-1980s with the introduction of supercomputers and vectorized explicit finite element codes.

The first period was essentially one of genesis and growth, a period of trial, of attempting to develop some understanding of an extremely complex structural mechanics problem. A variety of numerical techniques were applied to simulate the deformations, including folding and buckling of a car structure during the decisive first 50 to 100 ms of a crash test. Approximate solutions were obtained by spring-mass modeling of the vehicle [1,2], an approach originated in the aerospace industry. Alternatively, solutions were obtained by using beam element models in conjunction with nonlinear joint formulations [3,4,5] that proved very successful on numerous occasions, but required a relatively high degree of skill and experience from the analyst.

There were also attempts to obtain solutions based on first principles by modeling the car body as a continuum, and thus, automating the task of attributing discretized stiffness values to the structural components. Some of this work was based on quasi-static beam element formulation [6], implicit FE techniques [7,8,9], finite difference methods [10], implicit/explicit FE formulations [11] and, explicit FE time integration [12].

It appears that the first crash model [13] simulated a head-on collision of a vehicle front structure with a rigid wall, using the computer code DYCAST with an implicit solver [8]. In this model, the left half of the vehicle was represented by 504 membrane triangular, beam, bar, and spring elements. Haug [11] discussed the development of an implicit-explicit integration FE PAM-CRASH code, which was then applied to analyze the response of an A-pillar, and next to the right front quarter of a unit-body passenger vehicle structure. The quasi-static analysis was accomplished by an iterative incremental force/displacement analysis. The theoretical background for implicit FE formulation and an associated code for crash analysis were presented by Argyris et al [9]. The developed code was applied to calculate the impact response of a vehicle front structure, devoid of engine, transmission and driveline, when it impacted a rigid barrier from an initial velocity of 13.4 m/s. The solution accounted for material strain hardening and rate effects, and provided structural deformations. Other than the three examples mentioned above, the application of implicit FE solvers to crash analysis did not proceed beyond that point, primarily due to its inability to account for contact and folding of thin sheet metal structures and due to excessive demands on computer hardware storage and speed.

Some of these developments already contained the essential features that make up the core of any crash analysis software today. They combined time integration

with shell elements, node-to-segment contact force transmissions, and plane stress elasto-plasticity. Since these are still the basic algorithms used in today's analysis environment, it is not surprising that as early as 1973, very good analytical results were obtained on vehicle substructures. The continuum approach, however, remained mainly in the province of research, since the goal of full-vehicle simulation could not be achieved with sufficient accuracy due to the limited number of shell elements that could be handled by state-of-the-art computers before the mid-1980s. The resulting coarse meshes did not allow a representation of the global buckling modes in a full-vehicle model. Due to the high degree of interaction between the different panels of an automobile structure, it is necessary to consider the full vehicle in a single model to predict the energy absorption of the individual parts during a crash. The inability to fulfill this requirement brought the continuum approach and thus, the finite element approach, to automotive crash simulations to a standstill in the late 1970s and early 1980s.

The second period of development began in 1985 and continues to the present. It can be characterized as a period of rapid growth in both explicit finite element technology development and applications to progressively more complex vehicle structures. The breakthrough of finite element methods in this field and their consequent implementation in the design process of vehicles happened in the mid-1980s [14-17]. During these years, vectorized supercomputers were introduced to the industry, allowing explicit finite element technology to establish itself as the leading numerical technique for crashworthiness calculations of vehicle structures. These few crucial years paved the way for the rapid and dramatic evolution in the following decade, when analytical tools evolved from the research environment to an integrated and essential part of the vehicle design process.

Although similar processes occurred roughly simultaneously in Japan [18], the United States [19], and Europe [20], the first writing about application of explicit FE technology to crashworthiness of actual vehicle structure was published by ESI in 1985 [21]. ESI modeled the front vehicle structure of a VW POLO impact into a rigid barrier, from an initial velocity of 13.4 m/s. The FE model simulated the structure by 2,272 shell and 106 beam elements. An elastic-plastic constitutive model with strain hardening was used to describe the sheet metal behavior. The analysis provided vehicle kinematics and barrier force-time pulse. Subsequent to this simulation, automotive manufacturers have attempted many crashworthiness calculations. This chapter focuses on the efforts of the German automotive industry to develop an analytical capability, primarily due to one of the authors' involvement in these developments.

The genesis of the VW POLO model can be traced back to the Forschungsgemeinschaft-Automobiltechnik (FAT) committee of Germany. The

TABLE 3.1.1 **Computer runtime**

Hardware platform / software	Runtime for 80ms crash simulationon the Volkswagen Polo model
VAX-750/PAM CRASH	2000 hours
Cray-1 (scalar code)	100 hours
Cray-1 (vectorized code)	24 hours
Cray-1 (optimized code)	12 hours

FAT is a joint research committee of the German automotive industry, formed in 1983 as a working group. This group included all seven German automotive assemblers: Mercedes-Benz, Porsche, BMW, Audi, Volkswagen, Opel and Ford of Germany. The objective was to investigate the potential of the finite element method to predict the buckling behavior of an automotive car body during an overnight computer simulation. It is important at this point to note that two goals were set: accuracy and efficiency. Accuracy, and thus, the sufficiently realistic prediction of the vehicle's deformation mode, was not considered a complete result by itself. It was clearly realized that the industrial use of this methodology would depend mainly upon efficiency; that is, the ability of the analyst to provide a result within reasonable deadlines. Two projects commissioned by the FAT committee were executed concurrently during the next 2 to 3 years. The two contractors were IABG of Munich and ESI of Paris and Eschborn. They built finite element models of the BMW 300 and VW Polo respectively. Both models were based on quadrilateral shell elements and very similar in size as well as in concept. The model sizes of 6,000 to 7,000 shell elements were minimal compared to today's standards.

After a number of initial iterations, the research in both companies converged toward the use of explicit finite element methods due to the high convergence of problems observed when using implicit integration techniques to solve these highly nonlinear problems. Using explicit element-by-element techniques showed that the problem could be solved, at least in principle, although the computer runtimes involved were initially prohibitively high. Table 3.1.1 illustrates the dramatic changes that took place in the engineering hardware environment in the course of this project:

Two thousand hours represents roughly three months of continuous computation. This would obviously render all results obsolete in any modern design process, even before the results were obtained. Additionally, it is unrealistic to expect three months of continuous functioning of any hardware, due to hardware and software maintenance requirements. The performance of such a simulation thus required substantial effort by the analyst for management of results, restart data and other factors.

Although the transfer of the problem to the Cray supercomputer brought a spectacular improvement, runtimes of nearly one week could not be considered satisfactory, and had to be improved by other means. Vectorization of the software (PAMCRASH and CRASHMAS for ESI and IABG, respectively) and consequent optimization with respect to the particular features of the Cray-1 hardware ultimately allowed for runtimes that satisfied the original FAT overnight performance criterion.

Both projects were successful, resulting in a number of publications [22-24] which boosted the use of explicit finite element techniques in crashworthiness engineering in Germany and worldwide. Other European car companies had started working along the same lines independent of the FAT effort [25], contributing to the remarkable initial success of this methodology.

Since 1986, the development of simulation technology for crashworthiness has been spectacular, but industrial rather than technological in nature. It is instructive to compare the role of numerical simulation (based on explicit finite element methods) concerning crashworthiness engineering in an automotive company today to what it was in the mid-1980s. In the late 1980s, numerical simulation was almost exclusively a research activity involving very few engineers, and hardly affecting the design cycle. These simulations focused on frontal car-to-barrier crashes.

Today, car manufacturers are faced with numerous restraints dictated by different governments, in-house safety criteria, due care issues, and consumer-driven requirements that must be met before a new car is introduced to the world market. Corresponding to a variety of collision scenarios, 15 to 20 full-scale vehicle tests may be performed on a prototype. For example, to meet frontal crash requirements, a world vehicle's performance is assessed in a 30 mph crash into a full rigid barrier at 0 degree, +30 degrees, and -30 degrees. A similar test at 0 degrees from 35 mph into a full overlap rigid wall is run to assess NCAP performance. In addition, offset tests where the vehicle is run into partial overlap, deformable or rigid

barriers are conducted. These tests are in addition to air-bag deployment and immunity tests.

In addition to frontal impact performance, the industry must consider U.S. side impact, European side impact, rear impact, and rollover protection requirements. In short, the regulatory environment has mushroomed in the last decade. Added to this list are the competitive pressures to shorten the development cycle. In view of all this, it is obvious that the testing capacity with the automotive assemblers (and their suppliers) had to answer to a considerable growth in demand during this constantly reduced development cycle.

Numerical simulations have taken up a substantial part of the increased workload of crashworthiness engineers. The potential of simulations due to the constant and spectacular development of hardware and software as well as the accumulated experience of a rapidly growing number of analysts has evolved quickly enough in order to enable analysis groups to become fully integrated in the vehicle design cycle. Indeed, it would be difficult to conceive of vehicle design with today's constraints of regulations and safety on one hand, and competitive pressure on the other hand, without any simulation at all.

It is important to note that numerical simulations have not lowered the normal workload of the test laboratories in the least if this workload is considered as the verification and certification of vehicle prototypes. The contribution of simulation lies in that it complements a testing facility by preventing unnecessary work from being done. The strength of simulation lies in rapidly performing important simulations in the form of parametric studies that allow quick elimination from prototyping those designs which have a high probability of not satisfying the testing criteria. The ideal picture is indeed one of a design, heavily supported by analysis, resulting in building of only those prototypes that are almost certain to pass all final verification testing. This type of mainstream use of numerical simulation as a direct support for the design team requires the rapid development of full vehicle FE models at the very early stages of the design. In fact, FE crashworthiness models are, in today's design environment, the very first numerical models of a prototype to be completed. It is the building of these models that constitutes the most important bottleneck in the analyst's work plan.

Although it is generally believed that the usefulness of simulations for car design decreases rapidly as the design stage becomes more advanced and the type of design changes that influence safety become increasingly expensive, there is a role for simulations in later, and even ultimate, design stages.

When a safety-related problem appears in a prototype during a test, it is simulation that allows for diagnosis of the cause of the problem and selection of an appropriate structural modification in a minimal amount of time.

Finally, it must be mentioned that numerical simulations have found their way into each aspect of traffic safety-related engineering, although the above-mentioned design support work is certainly its main function. In addition to structural analysis, occupant simulation is increasingly performed using finite element models [26]. Simulations are used extensively by legislative bodies to support the development of new regulations [27] and for the improved design of roadside hardware [28].

From the previous discussion, it is clear that numerical simulations enabled the car companies to comply with an otherwise impossible escalation of the regulatory environment. Only the extensive use of numerical simulation has enabled the motor vehicle industry to introduce increasingly safer cars and trucks in less time without a corresponding increase in test facilities.

3.2 Overview of Explicit FE Technology

FE crashworthiness analysis of transportation vehicles in general, and of ground vehicles in particular, is among the most challenging nonlinear problems in structural mechanics. Vehicle structures are typically manufactured from many stamped thin shell parts and subsequently assembled by various welding and fastening techniques. The body-in-white may contain steel of various strength grades, aluminum and/or composite materials. During a crash incident, the structure experiences high impact loads which produce localized plastic hinges and buckling. This can ultimately lead to large deformations and rotations with contact and stacking among the various components. The deformations initially involve wave effects, associated with high stresses. Once these stresses exceed the yield strength of the material and/or its critical buckling load, localized structural deformations occur during a few wave transits in the structure. This is followed by inertial effects, which dominate the subsequent transient response. Of particular interest here are structural integrity and associated kinematics and stacking of components, forces transmitted through the various members, stresses, strains, and energy absorption. In addition, the crash event may be considered as a low- to medium-dynamic event (5-100 mph), in comparison with ballistic impact, persisting for a short duration of 100-200 ms. Closed-form analytical solutions for this class of problems in structural mechanics present a formidable

challenge to the analyst. Numerical techniques, at this time, appear to be the practical option.

The FE method of structural dynamics solves numerically a set of nonlinear partial differential equations of motion in the space-time domain, coupled with material stress-strain relations along with definition of appropriate initial and boundary conditions. The solution first discretizes the equations in space by formulating the problem in a weak variational form and assuming an admissible displacement field. This yields a set of second order differential equations in time. Next, the system of equations is solved by discretization in the time domain. The discretization is accomplished by the classical Newmark-Beta method [29]. The technique is labeled implicit if the selected integration parameters render the equations coupled, and in this case the solution is unconditionally stable. If the integration parameters are selected to decouple the equations, then the solution is labeled explicit, and it is conditionally stable. Earlier developments in nonlinear FE technology used primarily implicit solutions [30]. FE simulation for structural crashworthiness by explicit solvers appears to be first introduced by Belytschko [11]. Later, Hughes et al [31] discussed the development of mixed explicit-implicit solutions.

The explicit FE technique solves a set of hyperbolic wave equations in the zone of influence of the wave front, and accordingly does not require coupling of large numbers of equations. On the other hand, the unconditionally stable implicit solvers provide a solution for all coupled equations of motion, which require assembly of a global stiffness matrix. The time step for implicit solvers is about two to three orders of magnitude of the explicit time step. For crash simulations involving extensive use of contact, multiple material models and a combination of non-traditional elements, it turned out that explicit solvers are more robust and computationally more efficient than implicit solvers.

3.2.1 Formulation

The discretized equations of motion for explicit FE formulation can be written as:

$$\underline{M}\,\ddot{\underline{x}} = \underline{f}^{(ext)} - \underline{f}^{(\mathrm{int})} \tag{3.2.1.1}$$

where $\underline{M}$ is the inertia matrix of the structure, $\ddot{\underline{x}}$ is the nodal acceleration vector, $f^{(ext)}$ is the external force vector and $f^{(\mathrm{int})}$ is the internal nodal force vector.

Time integration of equations (3.2.1.1) are obtained by a central difference wtechnique (explicit integration) as follows:

$$\begin{aligned}
&\ddot{\underline{x}}^{(n)} = \underline{M}^{-1}\left(\underline{f}^{(ext)(n)} - \underline{f}^{(\mathrm{int})(n)}\right)\\
&\dot{\underline{x}}^{0.5(n+1)} = \dot{\underline{x}}^{0.5(n-1)} + \ddot{\underline{x}}^{(n)}\,\Delta t^{(n)}\\
&\underline{x}^{(n+1)} = \underline{x}^{(n)} + \dot{\underline{x}}^{0.5(n+1)}\,\Delta t^{0.5(n+1)}\\
&\Delta t^{0.5(n+1)} = 0.5(\Delta t^{(n)} + \Delta t^{(n+1)})
\end{aligned} \qquad (3.2.1.2)$$

where n is the integration step, Δt is the time step, $\dot{\underline{x}}$ and $\underline{x}$ are nodal velocity and displacement vectors , respectively.

Using the initial conditions, the nodal kinematics can be computed. Next, compute the strain rate, spin and Jaumann stress rate for each element:

StrainRate :

$$\dot{\underline{\varepsilon}}^{(n)} = 0.5\left(\underline{\nabla} \dot{x}^{(n)} + \underline{\nabla} \dot{x}^{(n)T}\right)$$

Spin: (3.2.1.3)

$$\underline{\omega}^{(n)} = 0.5\left(\underline{\nabla} \dot{x}^{(n)} - \underline{\nabla} \dot{x}^{(n)T}\right)$$

Jauman Stress Rate:

$$\nabla \underline{t} = \underline{C}\,\dot{\underline{\varepsilon}}$$

then, update the Cauchy stress for each element:

$$t_{ij}(t+\Delta t)=t_{ij}(t)+\dot{t}_{ij}(t)$$
$$Where\ \dot{t}_{ij}=\nabla t_{ij}+t_{ik}\omega_{kj}+t_{jk}\omega_{ki} \qquad (3.2.1.4)$$

then the solution proceeds to the next time increment and so on until the desired solution time is reached.

3.2.2 Explicit Integration

As can be seen, the explicit integration method stands for a numerical technique to integrate a system of ordinary differential equations that usually results from the spatial discretization of a continuum. "Explicit" refers to a specific technique whereby the equilibrium is expressed at a moment in time where the displacements of all spatial points are already known. Accelerations are determined from the equilibrium, and a central differencing technique allows the analyst to determine the displacements at the next timestep and repeat the process. The technique's attractiveness is that since the displacements are known at the time for which the dynamic equilibrium of the system is solved, this process requires the only inversion of the mass matrix, *M*.

Clearly, if a lumped-mass approach is used, the mass matrix is diagonal and no matrix inversion is necessary. This results in a very fast algorithm, since a system of uncoupled equations is all that needs to be treated. In all practical implementations, the internal forces are calculated using an element-by-element approach, thus avoiding the assembly of a global stiffness matrix and resulting in an algorithm with minimal central memory ('core') requirements. If carefully implemented, explicit integration is second order accurate. It is the element-by-element nature of the explicit algorithm that allows for the best characterization of this solution technique. Since stresses are calculated in each element separately from the corresponding nodal displacements and/or velocities, each timestep simulates the effect of the loads on one side of the element upon the opposing sides, thus representing the stress wave propagation through the element. The only drawbacks of the explicit algorithm are the conditional stability and the clear inability of the methodology to treat static problems. The conditional stability of

the explicit integration algorithm means that the integration timestep must be smaller then or equal to an upper bound value given as the Courant condition:

$$\Delta t \leq \frac{l_c}{c} \tag{3.2.2.1}$$

saying that the analysis timestep should not exceed the smallest of all element timesteps determined by dividing the element characteristic length through the acoustic wave speed through the material of which the element is made. The requirement is equivalent to saying that the numerical timestep of the analysis must be smaller than, or equal to, the time needed for the physical stress wave to cross the element. For typical automotive applications using mild steel elements (c= 5000 m/s) with a characteristic length of 5 mm, this results in an analysis time step of 1 microsecond. Due to this restriction, it is clear that explicit methods are best suited to treat problems of short duration and thus, high loading velocity and problems of a highly nonlinear nature that require small timesteps for accuracy reasons. It is again the rapid hardware development in the mid-1980s that has propelled automotive crash, a 100 ms phenomenon, in the realm of explicit analysis.

3.2.3 Shell Element

The shell element that has been, and still remains, the basis of all crashworthiness simulations is the 4-noded Belytschko and Tsay shell. [32-34]. Because this is a bilinearly interpolated isoparametric element, the lowest order of interpolation functions available is used. The element is underintegrated in the plane: there is a single integration point in the center of the element. Treatment of elasto-plastic bending problems is made possible by the definition of a user-defined number of integration points through the thickness of the element, all placed along the element normal in the element center. For computation, the use of an underintegrated formulation is very efficient. In most cases, it is faster to compute four underintegrated elements than it is to treat a single fully integrated element with four integration points. This is due to certain symmetries in the strain-displacement matrix that arise in the case of underintegrated finite elements.

The use of low order interpolation functions and a single in-plane integration point are the main reasons for the remarkable computational efficiency of the Belytschko and Tsay shell element. The drawback of the underintegration is that a number of zero-energy or hourglass modes exist in the element. Due to the simplifications in the evaluation of the element strain-displacement matrix, certain deformation modes result in a zero-strain calculation, and consequently, no stresses and nodal forces are calculated. This means that the nodal velocities can easily and rapidly diverge towards infinity as long as they remain parallel to the hourglass

modes of deformation of which there are six in the Belytschko and Tsay element. Hourglass instability is the major drawback with the Belytschko and Tsay shell element, or any other underintegrated element.

Hourglass instabilities are prevented mainly by the use of perturbation hourglass resistance techniques [35, 36]. This consists of detecting the presence of the hourglass mode in the element deformation pattern, and consequently, applying an external force field to ensure that the corresponding velocities and/or displacements remain bounded. It cannot be stressed enough that the hourglass forces result from an artificial external force field and do not form equilibrium with stresses in the material, consequently they tend to remove kinetic energy from the structure in a non-physical way.

The element formulation and integration techniques are chosen in a way to optimize computational efficiency, thereby compromising the material stiffness in the hourglass modes and the continuity of the out-of-plane displacement across the element boundaries.

Two additional features add to the amazing performance of this element. First, a co-rotational local system is used to ensure objectivity. All element strains and stresses are calculated in a local reference system that follows the element normal and the element 1-2 side. This ensures objectivity in the sense that no spurious strains and stresses are calculated if the element is subjected to large rigid body rotational motions. However, the position of the element local reference system depends upon the nodal numbering of the element, since it explicitly follows the element 1-2 side. This limits the validity of the formulation to problems involving small shear deformations. In practice, this is not a problem for solving crashworthiness problems since no large membrane shear deformations occur in sheet metal. It may cause hourglass modes to appear due to exaggerated rotations of the stress tensor.

Secondly, the element formulation is based on a strict uncoupling of membrane and bending effects. The membrane strains and stresses are calculated as resulting from the loads parallel to the local x-y plane exactly as in a plane stress element. The formulation is usually limited to small bending strains since no thickness changes of the element are considered. Again, this is not a problem when dealing with the simulation of sheet metal deformations. Bending stresses result from loading along the local z-axis and bending moments around the local x and y-axes. The bending strains in all integration points away from the element midplane are calculated using the Reissner-Mindlin equations and thus the assumption is made implicitly that the element is flat. In other words, all four nodes are in the same plane and a single normal is valid for the entire surface of the element. The

Belytschko and Tsay shell element is thus the sum of a plane stress membrane element and a Reissner-Mindlin plate element. Clearly, this is not valid if the element is warped. In a warped element, loads parallel to the local x-y plane cause bending strains and these strains are missed by the current element formulation. Consequently, warped Belytschko and Tsay elements severely underestimate the structure's bending stiffness. This is why this element fails the twisted beam test often cited in the literature.

In spite of a number of choices that clearly include a loss of generality and tradeoff for numerical robustness and computational efficiency, the results obtained using the Belytschko and Tsay element in thousands of crashworthiness simulations during more then a decade have been good enough to establish its usefulness to the industry. This can be explained in part by the particular nature of automotive crash events. Essentially, plastic hinges develop very rapidly over the full section of the thin (roughly 1 mm) sheet metal followed by large rigid body rotations of the parts between the hinges. Objectivity of the element is thus the primary requirement, and this is fulfilled in the element formulation. As long as the time for the development of the individual plastic hinges is small compared to the duration of the global event, the bending stiffness plays a less important role. Also, the small membrane deformation behavior and buckling behavior of the sheet metal is in line with the assumptions of the Belytschko and Tsay shell. Triangular elements were obtained by arbitrarily collapsing two nodes of a four-node shell element. This can result in a very inaccurate element, depending upon the shape of the triangle.

3.2.4 Plasticity

The plane stress plasticity at the individual integration points of the element is based on the membrane components of the stress tensor only. The yield condition is then written as follows for each integration point:

$$\sigma_{xx}^2 + \sigma_{yy}^2 - \sigma_{xx}\sigma_{yy} + 3\sigma_{xy}^2 \leq \sigma_y^2 \qquad (3.2.4.1)$$

where the yield stress is a function of the equivalent plastic strain and the strain rate in one way or another. After performance of an elastic stress update the yield condition is checked, and if it is not fulfilled, the stresses must be scaled back to the yield surface. Here, care must be taken to account for the nature of the plastic deformation and thus a flow of the material at constant volume must be simulated. Usually, a Newton iteration technique involving the unknown through-the-thickness strain in the element is performed. A non-iterative, radial return approach will lead to a deformation pattern involving a non-zero volumetric plastic strain. In fact, the apparent Poisson coefficient of the material during plastic deformation

will be equal to the elastic Poisson coefficient. Still, this computer-time-saving approach has been implemented in most explicit finite element codes and the approximation does not seem to have a very negative effect upon results of crashworthiness simulations, a further indication for the generally small deformation nature of the problem.

3.2.5 Contact Treatment

Finally, the code must provide for a means to simulate the transmission of forces between the individual body parts through contact. This is done by making contact interaction definitions part of the model or part of the spatial discretization. All early contact algorithm implementations were node-to-segment contacts: a well-defined set of nodes is not allowed to penetrate an equally well-defined set of segments (defined as either shell elements or sides of brick elements). If the nodes and segments are on different physical surfaces, a so-called master-slave contact definition exists. If they are on the same physical surface, a so-called single surface contact definition exists where the nodes of the surface are not permitted to penetrate the shell elements that they define. As previously stated, the contact definitions are an indispensable part of the spatial discretization of the structure. The definitions consist of a number of "contact springs" or spring elements that are generated in the model as soon as a penetration is detected and automatically deleted from the model as soon as that very penetration has been annihilated. The stiffness of this contact spring is given a default value by the software, but ultimately controlled by the user, who multiplies this default value with a penalty factor.

Clearly, users tend to increase the penalty factor in order to avoid deep penetrations and, consequently, unrealistic simulation results. However, an upper bound to the contact stiffness must always be considered since otherwise, the conditional stability of the explicit integration algorithm could be violated and instabilities could result. The default values of contact spring stiffnesses have been selected such that they operate just under the stability limit for a contact between two surfaces with identical (elastic) material properties and equal mesh densities. A contact spring operating at the stability limit will stop penetration of the slave node through the master segment in a single timestep. The penetration in a typical crash analysis where nodal velocities are of the order of 10 m/s is:

$$10*0.000001=0.000010m=0.01mm \tag{3.2.5.1}$$

showing that a safety factor of 10 with respect to the stability limit should not cause any appreciable loss of accuracy due to penetrations intrinsically allowed by the nature of the contact algorithm.

The main problems in contact algorithms originate in the node-to-segment nature of the model definition, as well as in the search algorithms that define which nodes are in contact with which segments. In particular, treating node-to-segment conditions only leads to a systematic failure of detecting edge-to-edge or edge-to-segment penetrations. Early search algorithms detected a nearest master node for each slave node and selected a single nearest master segment from all segments connected to the nearest master node. This is an algorithm that works very well for the simulation of the contact of two smooth convex surfaces, but fails in many situations that occur in the high curvature failure modes of an automotive structure. In particular, multiple impacts may occur simultaneously, and high curvatures in the mesh, as well as irregular meshes, may easily lead to the detection of a wrong neighbor segment, allowing numerous penetrations to remain undetected. Additionally, the search of the nearest neighbor node remained the most inefficient and time consuming part of the explicit solvers for many years, even after the introduction of the bucket sort algorithms.

3.3 Models Development Between 1987 and 1997

Between 1987 and 1997, the state-of-the-art model size for a full vehicle crashworthiness model has grown by a factor of 15, from 10,000 to 150,000 elements. The vast majority of this high number of elements are in the model of the vehicle body-in-white. All other car components are usually represented in much less detail, since their energy absorption is considered less important. It is generally thought that in the future, homogeneous models will be built in order to cover all load cases for frontal, side and rear impact simulations by a single model, saving roughly half of the expense of model development. The mesh size for this uniform and multi-load case model is between 5 and 10 mm. Mesh sizes larger than 10 mm do not provide enough accuracy, which mesh sizes below 5 mm make the element size smaller than the spot weld connections, in which case, another approach (brick element modeling) would make more sense. If the total sheet metal surface of a body-in-white is about 25 square meters, it is expected that model sizes between 250,000 and 500,000 elements for a full body-in-white would be the limit that should sensibly be used with shell elements. Each element represents between 0.5 and 1 gram of steel.

A further impression of the nature of this spectacular evolution can be obtained from Table 3.3.1 provided by Dr. Hannes Moeller of DaimlerChrysler Corporation:

TABLE 3.3.1 **Evolutuon of modelsize and CPU from 1988 to 1998**

Year	Typical model size	Hardware platform	Single processor CPU-time
1988	8-10000	XMP	5-10
1990	15-20000	YMP	10-20
1992	30-40000	YMP	20-30
1994	60-80000	C90	30-40
1996	100-120000	T90	40-50
1998	140-160000	T90	50-60

The search for higher reliability of the numerical results is the reason behind this ever-increasing model size. The first requirement would be that the mesh is able to smoothly represent the deformed shape of the car body, including all the highly-curved buckles in the crashed sheet metal. As a first order requirement, five elements (half a wavelength) are necessary to represent the width of a buckle in order to enable representation of the deformed geometry. The simulation result, however, remains mesh-dependent, and the predicted accelerations and energy absorption will continue to change until mesh convergence is reached. This point lies between 10 and 16 elements per buckle depending upon the section size, section shape, sheet thickness and material properties.

But model size is only the first half of the story. In over a decade of gained experience, it has become clear that mesh and element quality are of utmost importance for the reliability of the result of a crashworthiness simulation. The evolution in this field has, upon close inspection, been more spectacular than the increase in mesh size. From a coarse and rough approximation of the car body geometry (containing many conscious violations of elementary finite element theory) as was the state of the art in the mid-eighties, it has evolved toward a highly precise and a rigorous approach. Indeed, it is possible to say that meshing for crashworthiness has become a profession in its own right.

Normally, every sheet metal component in the car body is meshed separately using CAD surface data. In order to become a precise model of the sheet in the midplane, offsets of the surface data are carefully performed. The sheet is then meshed in a regular way using meshlines that are as much as possible parallel and orthogonal to the incoming pressure wave and using triangles only where necessary. Triangles are thus found in areas of mesh transition or areas of high double curvature (warpage) only. At the assembly of the individual sheets, further offsets may be necessary in order to guarantee a minimum gap between all parts so that no initial penetrations are generated. These gaps are also necessary to ensure a good performance of the contact algorithms and avoid deep penetrations through the midplane of the opposing part.

Once this task of generating the geometrical model has been performed, connections (spot welds) must be generated without deforming the geometry of the flanges on the individual sheet metal parts. This task can be completed in a number of ways and currently no clearly superior method can be distinguished. Several automatic procedures to generate spot weld elements of different kinds are currently being developed by software vendors as well as by automotive companies. Some fundamental problems remain, however. One is the real rotational stiffness of the spot weld, which will be discussed in a subsequent paragraph. Another problem lies in the desire to make the spot weld element location independent of the finite element mesh on both flanges. Since flanges are currently meshed with two elements over the width, automatic generation of a regular pattern for the spot weld elements proves a rather elusive goal. Still, it should be appreciated that in a modern vehicle model, between 3,000 and 5,000 spot welds are modeled individually and roughly in their exact locations.

Although the car body model accounts for approximately 75 percent of the entire model, more and more care is been given to modeling of the many other vehicle components. First to be mentioned are structural parts such as the subframe, doors, hood and wings, which use roughly the same modeling rules as the car body.

Particular care must be given to the connections between car body and subframe, which are often realized by bolts containing rubber bushings. Whereas the modeling of the rubber parts would require a prohibitively fine mesh in the context of a full vehicle simulation, it is still necessary to correctly account for the relative rotations between the body-in-white and subframe which can severely influence the acceleration response calculated in the passenger compartment. Therefore, a rigid body connection as well as a spring element connection will both lead to erroneous results. It is necessary to correctly simulate the motion of the bolt in

the bushing using contacts between surfaces that simulate the presence of the incompressible part of the rubber.

The powertrain model contains models for the engine, transmission, driveshaft and engine mounts, including their rubber bushings. The goal of this submodel is the correct simulation of the engine and driveshaft kinematics in order to account for the possible contacts with structural parts later on in the crash event. To achieve correct kinematics, it is necessary to accurately model the mass, rotational inertia and center of gravity position of the engine and transmission block. Furthermore, the engine mounts must be modeled in a similar way to the subframe mounts. This has proven to be the decisive factor in determining the relative rotation between powertrain and body-in-white. A cylindrical shell model with 5 or 6 elements over the circumference is typically used to model driveshafts in order to simulate potential contacts with brackets in the car body. Spherical joints connect the driveshafts to the wheel knuckles and to the transmission block. In order to avoid small timesteps, rigid body definitions are usually superimposed on the powertrain subsystem models. In order to obtain smooth contact forces between engine block and structure, the external geometry of the engine block must be accurately modeled using elements of a size not much larger then the ones used for the car body.

All the main parts of the front axle are also modeled using shell elements starting from CAD surface or line data. For a typical McPherson front axle, this subsystem will contain detailed modeling of the wheel knuckle, suspension strut, lower control arm and stabilizer bar. The same remarks made in the description of the powertrain system remain valid here. A detailed shell model is necessary to ensure that all potential contacts with structural parts can occur in the model. This means that the stabilizer bar is modeled as a cylindrical bar with 5 or 6 shells over the circumference. If these elements have a very small dimension, mass scaling or other techniques can be used in order to prevent a dramatic decrease in the calculated stable timestep. Usually the rubber bushings in the chassis model are not modeled in detail, as is done for the subframe and engine mounts. Rather, a series of revolute, cylindrical and spherical joints provide the correct hinges in the connections between the chassis parts as well as between chassis and car body structure. Obviously, a similar strategy is employed to model the rear axle parts in the case of rear impact simulations.

The wheels are connected to the axle models. The wheels consist of detailed geometrical models for wheel rim, brake disk and outer tire. The wheel rim and the brake disk are usually rigidly connected to the wheel rim, thus preventing the wheel from rotating. This must obviously be improved if mishandling simulations are performed, but is acceptable for crash simulations. A detailed model is

necessary to account for the correct inertial response of the wheel. The wheel can become a major load path in offset or oblique frontal crash events. Therefore, the tire stiffness must be accurately simulated. The air in the tire is simulated using the airbag algorithms of the explicit codes, yielding the pressure of a constant amount of air in the tire as a function of the compressed volume, assuming isothermal or isentropic conditions. A remaining problem is in the material model of the tires themselves. Existing tire models are far too complex to be incorporated in full vehicle crash models, and research is needed to generate reasonable and efficient approximations.

The third primary system to be modeled for a full vehicle simulation is the steering system including the steering rack, steering column and steering wheel. For the steering rack and its connections to the wheel knuckle, the same remarks are valid as for the modeling of the front and rear axles. A correct modeling of outer contours releasing the correct degrees of freedom in the connections using joint and/or spring elements is usually considered sufficient. Rarely, a detailed model is built that couples the translational motion of the steering rack to the rotation of the wheels. This can be of importance in the study of frontal offset and oblique impacts. Very often, a steering rack model that is fixed to the subframe structure is used, thus effectively blocking the wheel rotation. The steering column is usually modeled as a set of cylindrical tubes sliding in each other. It is this sliding motion that simulates the telescopic deformation of the steering column as the dummy hits the steering wheel.

To simulate the Cardan joints in the steering column, the exact geometry of the device is usually modeled with contact algorithms automatically accounting for the so-called stop-angles.

Observation has shown that engine motion is crucial for the dummy response in the passenger compartment during a frontal impact. Engine motion, in turn, is at least partly determined by contacts with the structure and other components located under the hood. Consequently, these components must be modeled carefully and with mesh sizes that are not very different from the engine block mesh size. These components include the battery, radiator, air conditioning unit, automatic braking system unit, ventilators and electro-engines at the radiator, radiator bracket and light brackets. Some of these are mild steel structures and can be modeled as such. Others are hard points and little care must be given to the determination of their stiffness as long as the resulting strength is considerably higher than that of the surrounding structural parts. An exception is the radiator model, which must crush under the impact of the engine block and somewhat damp its acceleration response. Equivalent models based on force-displacement

curves determined in a drop test are usually used, since a detailed modeling of the radiator structure is again prohibitive.

Whereas a structural model of the doors is largely sufficient for the simulation of frontal and rear crashes, this is not true for the simulation of side impact load cases. In this case, the door inner components must be carefully modeled. Hinges and locks must be modeled in such a way that the correct rotational degrees of freedom are released between the door model and the model of the body-in-white. Door structures are mostly quite weak with respect to bending. The inner components such as guide rails for the window, electrical motors, loudspeakers and the window glass provide the flexural stiffness of the entire component, and thus, determine the critical timing of the impact between door and occupant. The inertial response of the door structure is important in determining the velocity of impact with the dummy. The mass of the door as well as the masses of its individual components should be carefully checked.

For completeness, the following modeled components for different load cases are mentioned. Windshield and bumper are modeled in frontal impact, whereas the fuel tank and spare wheel and tire are typically present in rear impact models. The instrument panel may be required for the simulation of frontal and side impact and the front seats are essential in all models. At this point, roughly 50 to 60 percent of the total vehicle mass is modeled and a careful mass check is typically performed at this stage. The remaining masses are traced and locally added to the model as density increases and/or nodal added masses.

The modeling technology has expanded beyond the actual vehicle models with finite element approximations of deformable barrier structures, crash dummies and different impactor devices.

3.4 Software Development Between 1987 and 1997

Modeling technology has evolved towards ever larger and more detailed numerical models of the vehicle in a quest for more accuracy and more reliability in the results. Software development has primarily fought a battle of trying to run and manage these models with continuously increasing size, using essentially the same basic technology. A first important focus point of development was on animation packages for rapid post-processing of the simulations. These packages allowed for visualization of the simulated crash event and the deformation modes of the car body and for display of plastic strain, stresses and energy densities over the individual parts. This allowed the engineer to immediately identify those components that absorb more or less energy. Similarly high emphasis was placed

on the interactive pre-processing software of the models. The main goal was to quickly incorporate structural changes in an existing numerical model.

The main programming effort has been to increase the efficiency of the solvers themselves. Explicit finite element codes have been optimized to the point that they run in a 99 percent vectorized mode. Although it must be said that the element-by-element nature of the codes lends itself particularly well for vectorized processing, this was certainly a remarkable achievement considering the nodal force assembly, and the search algorithms in the contact-impact routines. A similar, even more important effort is continuously displayed in the parallelization of the codes achieving ever better scaling performance on both shared memory and distributed memory machines. A major advance was the replacement of node-based contact search algorithms by so-called segment-based search algorithms. The old algorithms based on the search of a nearest master node for every slave node are always computer-time consuming even if bucket sorting improves this situation. With the new segment-based search methods, an algorithm was introduced that is not only computationally much more efficient, but also improves on many of the shortcomings of older algorithms.

Finally, a number of techniques were developed in order to allow explicit simulations to run with a constant timestep value. This at first seems a non-trivial matter since the stable time step of the analysis is linearly dependent upon the shortest mesh dimension in the model. As deformation changes (reduces) this dimension, a drop of the timestep seems mathematically unavoidable. Indeed it is not possible to keep a constant timestep during a crash simulation with highly deforming shell elements without changing the physics of the problem. Several methods were developed to achieve this. They vary from the so-called small strain formulations where the influence of the change in geometry upon the element stiffness is ignored from a certain point on (or during the entire analysis), to a controlled reduction of the material's elastic modulus as it plastically deforms. The most widely used method is mass scaling. As an element dimension decreases, the corresponding material density or nodal masses are increased in such a way that the resulting time step remains constant.

These options render crashworthiness simulations feasible and useful in about 75 percent of all cases. Although the physics of the problem are locally modified, this is not a major objection if one considers that the local stress distributions must have been wrong before mass scaling (or any of the other constant timestep options) was applied. Since a vehicle crash is by nature a small strain event, no large membrane strains should really occur in the shell elements that represent the car body. Consequently, the mesh dimensions should not change and the timestep should ideally be constant.

This is true only if the mesh is sufficiently fine in order to give a smooth representation of the deformed (crashed) vehicle geometry, including all high curvatures that may occur. This will in practice rarely be the case. Mostly, the mesh is at least locally too coarse, and large strains occur at the element level, resulting in a drop of the timestep. Apart from a non-realistic stress distribution, large deformations also violate the basic assumptions of the Belytschko and Tsay element and will mostly result in a locally unstable behavior or in the development of hourglass modes. It can then be said that the application of mass scaling has little or no influence on the resulting accuracy of the global simulation result.

The basic technology of explicit finite element codes as applied to crashworthiness problems remained largely the same during the last decade. One of the major improvements in accuracy was the replacement of degenerated quadrilateral elements by a true C0 triangle element as proposed by Belytschko [35]. This element is free of hourglass modes and has a bending response equivalent to the flat quadrilateral Belytschko and Tsay element. It constitutes a major improvement with respect to a degenerated quad but still must be used with care and in limited numbers mainly because of the in-plane shear stiffness that can be too high in certain cases, depending on mesh size and shape.

It must also be noted that a large number of special purpose options were added to the codes in order to fulfill crash-specific functions in the models. Such as rigid bodies, but spring elements, spot weld elements, joint elements and occupant simulation oriented options such as seatbelt, and airbag models. These mainly improve the application scope of the codes. It seems that the simulations have arrived at a crossover point where the factor limiting the accuracy of the simulation is no longer the mesh, but rather, the numerical algorithms that are used in the explicit finite element codes. Consequently, a clear trend can be observed towards the use of more sophisticated algorithms as will be explained in the Section 3.5 – Limitations of Current Technology.

3.5 Limitations of Current Technology

In the late 1980s, a leading engineer in the German automotive industry referred to crashworthiness simulations as “numerical adventure,” and it must be said that he was not wrong. To claim that early simulation work in this field was more of an art then a science is almost an understatement.

Any finite element simulation activity can be seen as a chain with two links. The first link is the numerical model, essentially a hyper-complicated mass-spring system whose dynamic behavior is an approximation of the continuum (the car) that is to be modeled. The second link is the software or the numerical algorithm that has to perform a numerical time integration of the system of ordinary differential equations that govern the behavior of the model. Again, the solution obtained on the computer is an approximation of the correct (analytical) solution.

The main problem with early simulation work was clearly the coarseness of the shell element mesh representing the car body. This resulted in simulation of the low curvature (high wavelength) buckling modes only, and thus constantly overestimated the energy absorption in the structure since high curvature modes were precluded from the simulation by the outlay of the mesh. Too coarse meshes generally resulted in too stiff behavior of the energy absorbing, highly deforming structural parts. The weak link in the chain was clearly the mode, and any additional loss of accuracy due to the use of very simple algorithms was almost welcome.

Some of the algorithmic deficiencies tended to compensate for the errors due to the coarseness of the finite element mesh. Penetrations allowed due to failing contact algorithms and zero energy modes in underintegrated shell elements would all weaken the structural response and thus improve correlation between the numerical and measured results.

Today, this situation has been reversed. Greater potential for improvement in the near future lies in the use of more accurate algorithms rather than in further refinement of the models. This is due to the continuous increase in mesh size and mesh quality and better representation of the real vehicle by the model through detailed modeling of multiple components. In other words, the algorithms have become the weak link in the chain. Improved algorithms for shells and contacts have been available in explicit codes for quite a while, but have not been used extensively for a variety of reasons, including increased computer time and lack of numerical robustness.

In the near to mid-future, current model sizes of roughly 150,000 elements for a single class of load cases (frontal, side or rear) and a homogeneous mesh of roughly 350,000 elements for all load cases could be a reasonable model size for all crashworthiness engineering purposes. This assumes that improved contact algorithms with edge-to-edge capability are used in conjunction with fully-integrated, or at least physically stabilized, shell elements. The required computer time is estimated to be three to four times more than current technology requires.

Approximately half of all numerical problems in modern crashworthiness analysis work are caused by edge-to-edge penetrations. In early explicit simulations (for example in the defense industry), this was never a problem since contacts between convex surfaces with low curvature were considered and consequently node-to-segment contact algorithms have more than sufficient generality to detect all occurring penetrations. This is no longer the case for automotive structures. The complex surfaces with high double curvature are discretized by somewhat too-large finite elements, resulting in a polygonal surface with lots of kinks and edges. Edge-to-edge penetrations can go undetected since they cause no nodal penetrations through any of the segments. This by itself should cause no further problems, except for making the model less stiff than the actual structure where no penetrations can occur. However, consequent movements of the penetrated segments can easily lead to so-called impacts of nodes on segments 'from the wrong side.' These contacts in tangled structures will lead to extremely high local contact forces since entire structural parts may be hung up upon a single node. Suanomalies in the models will lead to local instabilities, hourglassing due to the extreme out-of-plane loads and potentially abort the simulation prematurely. The only way out provided by classical contact algorithms is to set the tangled nodes free and allow penetration without any further checks resulting in a further loss of realism. Edge-to-edge algorithms are currently being introduced into all commercial explicit finite element codes.

A second improvement is the efficient neutralization of the zero-energy or hourglass modes in the shell elements. As explained in Section 3.2.3 – Shell Element, zero-energy modes exist in underintegrated shell elements and correspond to zero-element stiffness with respect to certain deformation modes, such as in-plane bending. The loss of stiffness caused by this approach was clearly offset by the gain in efficiency due to underintegration, and in any case, was not seen as a great burden as long as the use of coarse meshes resulted in a behavior of the model that is generally too stiff.

The use of increasingly finer models allows for detection of the influence of the zero-energy modes and the corresponding perturbation hourglass forces in the numerical models. The perturbation hourglass forces are nodal forces introduced numerically in order to prevent the hourglass velocity components in the element from becoming unbounded. Although these forces are supposed to make up for the missing element stiffness, they do not correspond to a stress in the element, and thus constitute an external force field of rather arbitrary magnitude controlled by user-defined coefficients. Due to the introduction of this force field, a perturbation-stabilized underintegrated element may behave both too weak or too stiff compared to reality.

A first possibility to cope with the problem seems to be full integration using four-Gauss integration points in the element of the bilinearly interpolated element. Unfortunately, this rather straightforward solution does not work. Fully underintegrated elements with uniform bilinear interpolation suffer from another drawback called shear locking. Shear locking occurs when non-zero out-of-plane shear strains are predicted by the element in conditions of pure bending resulting in an overly-stiff element response. This problem is caused by uniform interpolation: if out-of-plane deflections are interpolated with higher order rather then bilinear functions, formulations that exhibit no shear locking are possible. However, this dramatically increases the complexity of the implementation and decreases the element performance. Development of a fully-integrated element that avoids all shear locking and maintains the simplicity of uniform bilinear interpolation has proven to be a challenging task.

Several solutions exist to neutralize hourglass modes using uniform bilinear interpolation while avoiding shear locking. A first possibility is the selective-reduced-integration (SRI) elements. [37,38]. This solution consists of performing a full integration for the membrane and bending strains combined with a reduced integration for the out-of-plane shear strains. These elements effectively avoid shear locking for rectangular elements but some problems still occur in irregular meshes.

A second solution corresponds to the assumed-natural-coordinate-strain (ANS) elements. Here, the isoparametric coordinate field is no longer differentiated, but improved estimates of the out-of-plane shear strain field are used directly. This approach leads to a formulation without shear locking independently of the quadrature rule used and both reduced integration and full integration implementations exist in most commercial explicit finite element codes. Obviously, a reduced integration ANS element does not solve the original hourglass problem and would not suffer from shear locking. The advantage of the ANS approach for these elements lies in the improved accuracy obtained in irregular meshes. In particular, the ANS element passes the Kichhoff patch test, whereas elements with classical quadrature of the shear strains always fail this rather elementary requirement. A very efficient fully-integrated ANS element exists in the LS-DYNA code, which overcomes all hourglassing and shear locking problems at a cost of roughly three times the original Belytschko and Tsay shell element.

If full integration is still perceived as not efficient enough to allow parametric studies on large-scale crashworthiness models of vehicles, a more economical approach may be given by physical stabilization [39]. Here, underintegrated versions (preferably of the ANS element) are used and an approximate analytical integration is performed over the element of the non-constant part of the strain.

The constitutive law is invoked in order to estimate hourglass stresses resulting in a set of nodal forces that are supposed to correct missing stiffness components of the element rather exactly. This approach is much more efficient than full- or reduced-selective integration and requires only about 30 percent more computer time then the original Belytschko and Tsay element. The element also passes the Kichhoff patch test.

Next to the existence of zero-energy modes, a second potential problem with the highly efficient Belytschko and Tsay shell element is its limitation to flat geometries. This results from the use of the Mindlin plate theory where the fiber direction is assumed to coincide with the normal to the plate surface. If this assumption is used in warped elements, the bending strain can be underestimated for two reasons. First rotations normal to the element will not cause any curvature to be calculated although these rotations may not be parallel to the nodal drill degrees of freedom (fiber direction) in all nodes of the element. Second, force loads in the element plane should also cause bending strains in a warped element and will fail to do so when the unmodified Belytschko and Tsay element is used. Those effects will lead to the failure of the so-called twisted beam test by this element. An efficient coupling of membrane and bending deformation is advocated in [39]. These formulations allow accurate modeling of surfaces with double curvature using warped elements with warp angles up to 15 to 20 degrees.

It should be emphasized strongly that none of the improvements described above affect the original assumption that only small deformations exist within a single shell element. These improvements are merely meant to correct some deficiencies of the element formulations within this framework. Thus, the use of more sophisticated elements does not allow the use of coarser meshes. All rules developed earlier to determine mesh density of a crashworthiness model still apply. A good crashworthiness simulation can only be obtained if the mesh is able to smoothly represent the deformed geometry of the car body. In fact, this condition may have become stronger then before since large element deformations may lead to numerical problems and generate instabilities that were almost never the case with the numerically ultra-robust Belytschko and Tsay element.

3.6 Applications

This section presents a summary of typical FE models used in frontal crashworthiness analysis.

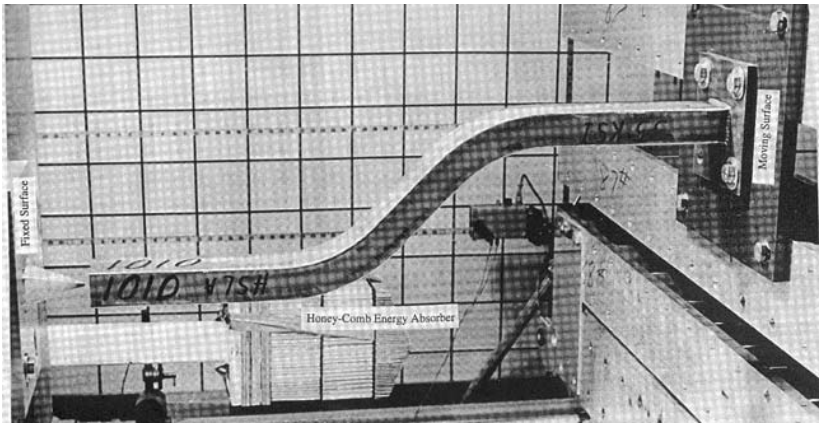


Fig. 3.6.1.1 **Rail test set-up**

3.6.1 Component Models

Component models can be grouped into generic components such as S-rails and rectangular tubes, and actual isolated components such as upper rails, lower rails and hoods. These components are typically tested in both quasi-static and dynamic modes to identify their crush performance. In dynamic testing, a drop-silo or a sled is used. In drop-silo testing, the component is fixed to the ground on a load cell and loading is typically applied from the gravitational fall of a rigid mass onto the free end of the component. In sled testing of components, the component is mounted horizontally onto the sled (Figure 3.6.1.1) which subsequently is launched to impact a rigid or deformable surface with the component making first contact. Figure 3.6.1.2 shows the S-rail final deformations corresponding to initial impact speeds of 2, 4.5 and 8.2 m/s into a rigid wall. The rail deformations exhibited two plastic hinges at the rail curvatures, rotation at the free end and plastic hinge at the fixed end. The measured peak force increased with impact speed from about 50 to 60 kPa, due to strain rate effects of the material used. The FE simulation corresponding to 8.2 m/s impact agreed quite well with the test result when the strain rate effects were included in the simulation. Increasing the number of shell elements from 2,000 to 3,000 showed minor influence on the overall response.

The deformed mid-rail shapes of an actual passenger car mid-rail are shown in Figure 3.6.1.3, corresponding to test speeds of 2.2, 4.4 and 6.7 m/s, respectively [40]. In Figure 3.6.1.4 the FE predictions of the force-time pulse show good a

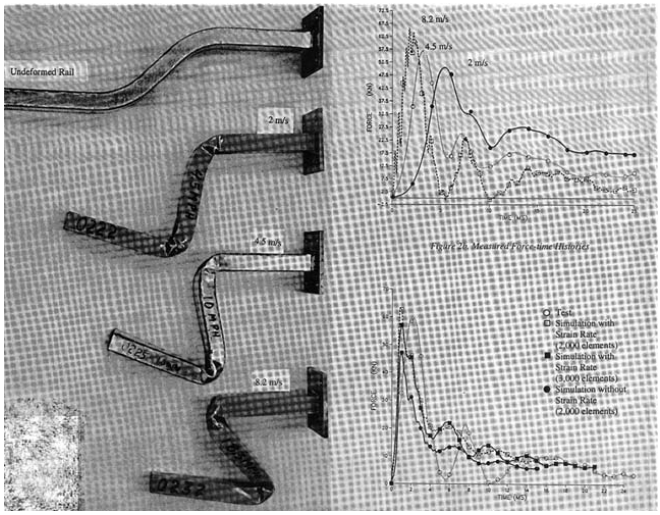


Fig. 3.6.1.2 **Rail response**

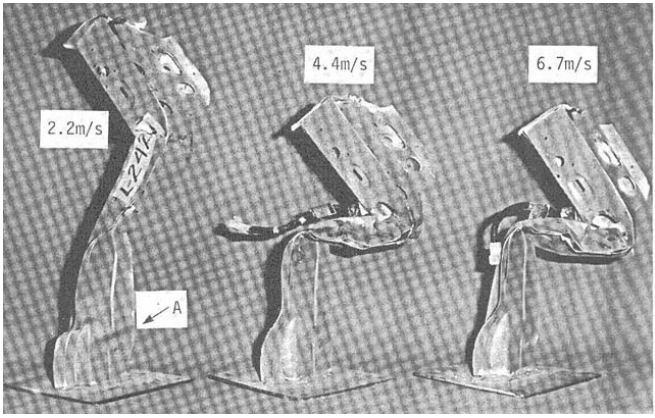


Fig. 3.6.1.3 **Vehicle component deformations**

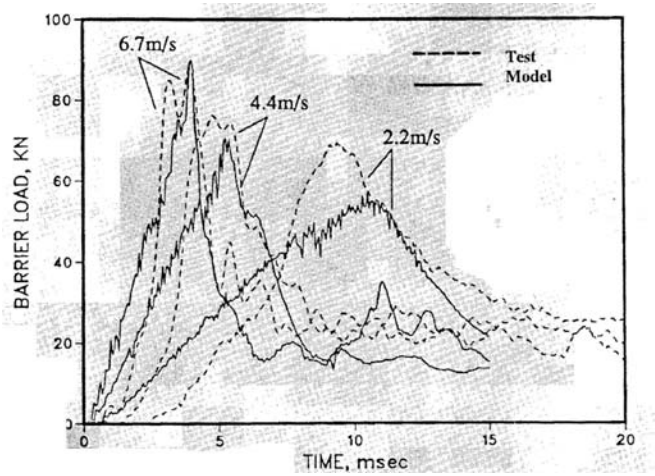


Fig. 3.6.1.4 **Measured and FE-calculated forces**

agreement with the test data. Like the S-rail response, the peak force increased with increasing the impact speed due to strain rate effects.

3.6.2 Substructure Models

A vehicle front structure subassembly finite element model is presented in Figure 3.6.2.1. Figure 3.6.2.2 shows a comparison between the predicted and measured force pulse from impact of a front structure subassembly into a rigid wall [41]. In this case, the impact speed was 13.4 m/s. In this simulation, no strain rate effects were included in the analysis since themid-rails were manufactured from high strength steel, which typically exhibits little strain rate effects.

3.6.3 Full-scale vehicle structure models

As indicated earlier, FE models of frontal crashworthiness have been evolving since the early 1980s. Table 3.6.3.1 provides a summary of representative front structure models, available in the open literature. These models simulated vehicle crash into a rigid wall. They clearly indicate the evolution of the models in size and complexity. It may also be observed that detail modeling of vehicle structures has become an integral step in the vehicle design process. Other frontal impact models include oblique (+/-30 degree) impacts with a rigid barrier, offset impact

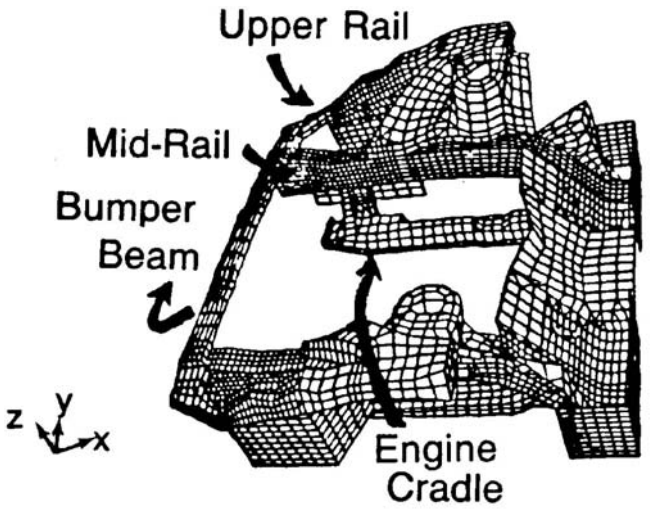


Fig. 3.6.2.1 **Vehicle front structure subassembly**

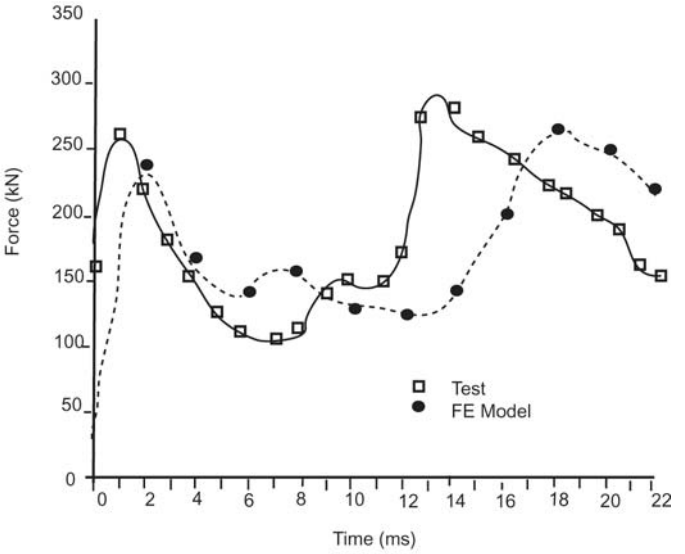


Fig. 3.6.2.2 **Force-time history**

Table 3.6.3.1 **Summary of typical frontal impact models**

Year/Ref	Mfr.	Elements	Sim.time (ms)	Analysis Code	CPU hours/ platform
1986 [42]	BMW	2,800	90	CRASHMAS	89/
1986 [19]	Suzuki	3,439	60	DYNA3D	24/Cray-XMP
1986 [43]	VW Polo	5,661	60	PAM-CRASH	4/Cray1
1986 [24]	Citroen (BX)	7,900	80	PAM-CRASH	12/Cray/XMP
1986 [25]	Opel (Vectra)	7,991	80	PAM-CRASH	16/Cray-1S
1987 [44]	GM (GM 80)	9,500	80	PAM-CRASH	12/Cray-XMP
1987 [18]	Isuzu (750 Coupe)	10,000	70	PAM-CRASH	14/Cray-XMP
1989 [20]	Saab (900)	7,500	80	DYNA3D	22/Cray-XM-P28
1989 [45]	Mazda	18,000	80	PAM-CRASH	18/Cray-XMP
1989 [46]	Nissan	12,000	120	PAM-CRASH	20/Cray-XMP
1989 [47]	GM (W Coupe)	17,000	80	DYNA3D	20/Cray-XMP
1992 [48]	GM	17,000	80	DYNA3D	9/Cray-YMP4
1994 [49]	Opel (Omega)	16,000	100	RADIOSS	—/Cray-YM-P4
1994 [50]	Ford (Windstar)	60,000	100	RADIOSS	12/Cray-C90-16
1996 [51]	GM (G Sedan)	62,235	100	DYNA3D	45/Cray YMP8E

models with rigid or deformable barriers with 40 to 50 percent overlap, vehicle-to-vehicle impact with full or partial overlap, and central or off-center impacts with a rigid pole.

The following example illustrates the development of a frontal crash model of a four-door passenger car. It simulates the primary load carrying components of the vehicle in frontal impact with a rigid barrier. Particular attention was paid to the FE mesh of the mid-rails, lateral rails, front tie bar, and dash panel. All sheet metal components were modeled and fastened together by spot welds corresponding to the actual hardware. Approximately 10 mm x 10 mm shell elements were used in the front structure where plastic hinges and buckling were anticipated. Coarser mesh was used for the structure behind the dash panel where limited deformations were expected. The model included a bumper system with appropriate connectivity to the mid-rails. The radiator was modeled using solid elements, with material properties corresponding to honeycomb behavior in compression. The engine and transmission were simulated by rigid shell elements, which represented the mass and moments of inertia at the engine's CG location. The engine mounts between the engine and the supporting structure were modeled by appropriate joints. The tires and wheels were modeled by a combination of shell and solid elements to represent the compliance and load transmission characteristics of these components. Two front door models were included with appropriate hinge properties. The rear doors were excluded, as their influence on frontal crash performance was assumed negligible. An instrument panel was also included along with appropriate structures for knee restraint. Finally, the inertial characteristics of the whole vehicle model were checked against the actual vehicle and concentrated masses were added to ensure agreement between the model's inertia and the corresponding hardware.

3.6.3.1 Model Statistics:

- 61,500 shell elements
- 500 solid elements
- 25 beam elements
- 1,200 spot welds
- 15 joints
- 40 concentrated nodal masses
- 10 springs
- 200 parts
- 66,000 nodes

3.6.3.2 Contact Definitions

A rigid wall was defined in front of the vehicle with stick condition. Automatic contact surfaces were defined in six zones as follows:

- Front-left corner (up to front body hinge pillar)
- Front-right corner (up to front body hinge pillar)
- Front-center (include up to the middle of the engine)
- Rear-center (from middle of the engine to the fire wall)
- Driver side center-pillar to door
- Passenger side center-pillar to door

3.6.3.3 Initial Condition

An initial velocity of 13.4 m/s was defined for the entire vehicle structure which impacted a rigid wall.

3.6.3.4 Results

The model response was calculated on a CRAY Y-MP8E system. The time step was approximately 0.7 ¼s. A 100 ms simulation was completed in about 45 hours on one processor. In this run, it was necessary to refine the radiator model since severe hourglassing was observed. The initial (at time 0) and final (at 100 ms) vehicle deformed shapes are shown in Figure 3.6.3.4.1. Intermediate vehicle configurations (not shown here) exhibited realistic sequential deformations as seen in high-speed film analysis of barrier crashes. The time histories of the global energy balance, velocity at the front rocker, and barrier force provided very reasonable results, comparable to test data [51].

In addition to frontal crash models, other models have been developed to simulate side impact with a deformable barrier [52], rear impact, and roof crush models, respectively [53]. Also, car-to-car crash models have been simulated [54].

3.6.4 Integrated Vehicle-Occupant-Restraints Model

Traditionally, frontal crashworthiness analysis has focused on sequential simulations of vehicle structures and occupants, with the occupant simulation being driven by the vehicle (calculated or measured) deceleration pulse. Consequently, analysis techniques and associated tools have been developed to meet the needs of the two communities. This process has many shortcomings, including real-time interactions between the occupant and vehicle structure during the crash event are not simulated, the analyst must learn and use two analysis

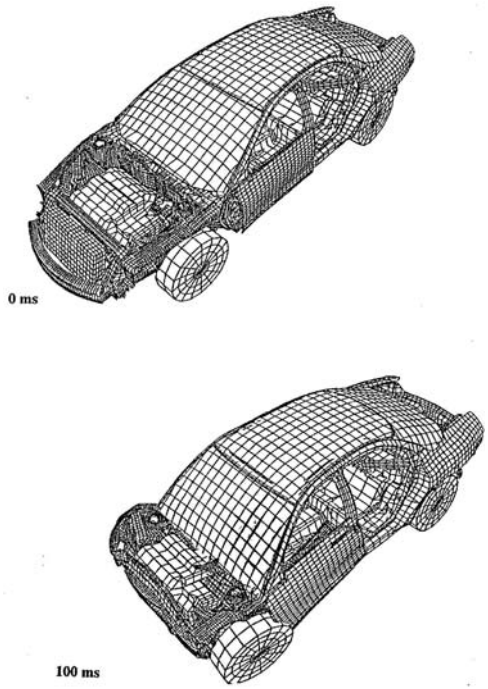


Fig. 3.6.3.4.1 **Initial and final vehicle deformations**

techniques which is an inefficient use of human and hardware resources. To remedy this situation, attempts have been made to couple occupant and structural codes [55]. This process allowed for real-time interactions between the vehicle and occupant, but left the analysis community to deal with two analytical tools.

It has always been, and still remains, the desire of safety analysts to simulate the crash event in one model that can predict occupant response associated with the crash event in real time. Conceptually, all FE codes can accomplish this task, since rigid body equations of motion are a special case of the FE formulation. The only missing components were dummy and restraint models. Once these are developed, crashworthiness simulations that include structures, occupants and restraint systems in one model become a reality. The development of a subsystem model of the Hybrid III thoracic dummy model interactions with a steering wheel using a single code has been demonstrated [56]. The Ove-Arup group discussed the advantages of using a single code in safety analysis, and presented graphics depicting dummy models and an integrated vehicle-dummy model [57].

Schelkle and Remensperger [58] discussed the development of an integrated model of a passenger compartment and occupant using a single FE code. The model simulated a sled test by 8,700 elements in frontal crash, and included an unfolded air bag, steering system, knee bolster and seat. A 100 ms simulation required 13 CPU hours on a CRAY-2 computer. Although the model exhibited reasonable kinematics, the authors indicated that the contact algorithms were not sufficiently robust to account for interactions between the dummy arms and the deploying air bag.

Khalil and Sheh [51] developed an integrated model for frontal crash. This model integrated the following components/subsystems into one FE model. These are the primary components of the model:

- vehicle including a body-in-white structure of a four-door passenger sedan,
- engine, transmission, etc., weighing 1,750 kg,
- bucket car seat structure with the seat cushion,
- nergy absorbing steering column with a steering wheel and folded air bag,
- instrument panel, including a driver side knee bolster,
- door structure, and
- Hybrid III dummy

Model statistics:

- 70,000 shell elements
- 9,000 solid elements
- 300 beam elements
- 1,300 spot welds
- 300 parts
- 91,000 nodes
- 20 contact segments

Figure 3.6.4.1 shows the integrated model at time 0 and a deformed configuration at 100 ms. The model kinematics, showing vehicle deformations, air bag deployment and forward motion of the dummy and subsequent interactions with the air bag and knee bolster are qualitatively similar to a barrier test (Figure 3.6.4.2). Figure 3.6.4.3 shows the energy balance for a typical run. It can be observed that the total energy remained approximately constant throughout the 100 ms duration, and the rise in internal energy and the decay in kinetic energy are smooth. This attests to very little interpenetrating among the contacted segments. The vehicle velocity response in time, at the rear rocker, is shown in Figure 3.6.4.4, along with experimental data from one test. The velocity trace agreed quite well with test data, particularly at the point where the vehicle velocity crosses the zero line.

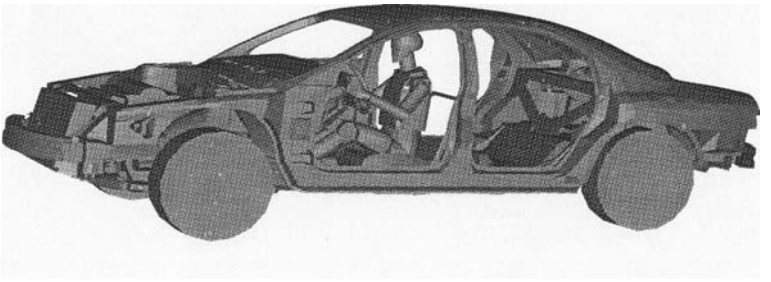


Fig. 3.6.4.1 **Integrated model**

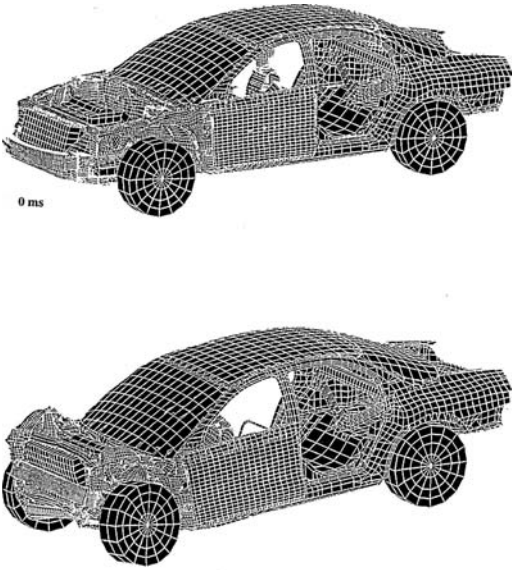


Fig. 3.6.4.2 **Integrated model deformations**

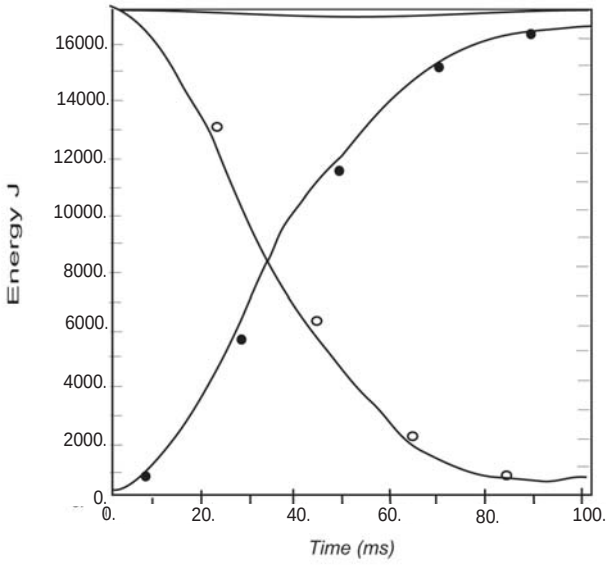


Fig. 3.6.4.3 **Energy balance of integrated model simulation**

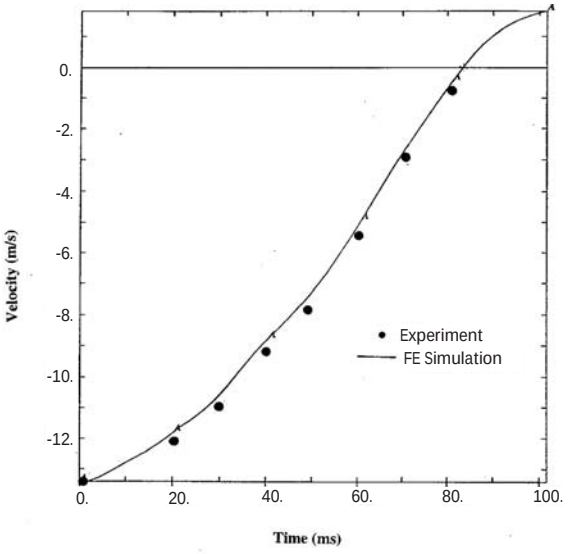


Fig. 3.6.4.4 **Rear rocker velocity**

This is of interest as it indicates that the model captured the overall stiffness of the deforming vehicle structure.

Figure 3.6.4.5 shows the barrier unfiltered force-time pulse. The pulse shape with its two peaks and the times at which they occurred is consistent with experimental data.

The first peak force almost coincided with the results obtained from one test. However, the second peak was only 60 percent of the test value. This may be due to inexact modeling of the engine-to-dash panel interactions.

Subsequent to development of the integrated model, to illustrate its robustness it was exercised to simulate an NCAP test. Figure 3.6.4.6 shows the model deformations at 100 ms corresponding to impact with a full rigid barrier from an initial speed of 35 mph.

Next, the model was exercised to simulate vehicle frontal impact with a rigid pole. The initial impact speed was 30 mph. Figure 3.6.4.7 shows the initial model set-up and the deformed configuration at 100 ms.

Finally, the model was tested to simulate vehicle impact with an offset rigid barrier. The initial vehicle speed was 30 mph. The vehicle impact was on the left side with 50 percent barrier overlap. The initial model configuration and deformed configuration at 100 ms is shown in Figure 3.6.4.8. A comparison of frontal vehicle deformations in time is shown in Figure 3.6.4.9, which clearly demonstrate the difference in frontal deformations corres-ponding to the previous four impact scenarios.

3.7 Summary

Although the FE technology for structural mechanics was introduced in the early sixties, it took about 25 years of additional development to apply it successfully to crashworthiness simulation of automobile structures. The developments were mainly in nonlinear problem formulation of shell elements, reduced spatial integration, explicit time integration, plasticity, and contact-impact treatments. The role of super computers and code vectorization was indeed indispensable for the development of full-scale vehicle models.

The mid-eighties to the mid-nineties time span can be characterized as the renaissance period of FE crashworthiness models. Generic and actual components of vehicle structures as well as full-scale vehicle models were developed to simulate

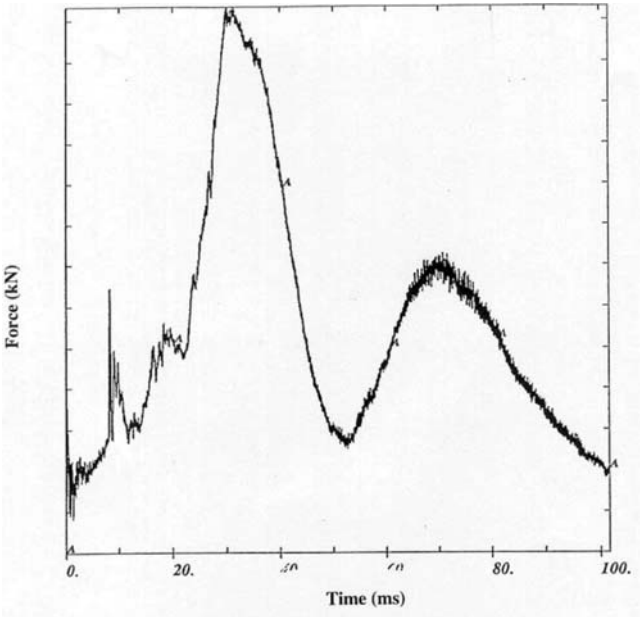


Fig. 3.6.4.5 **Force pulse of integrated model simulation**

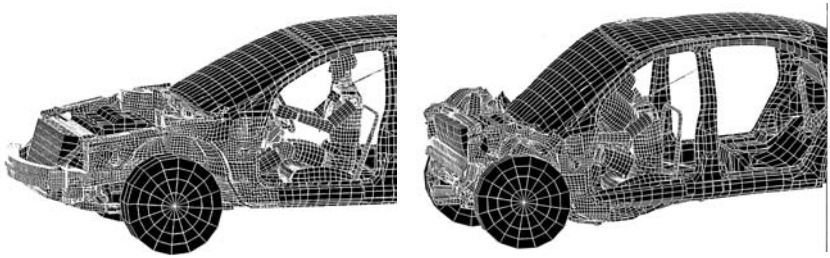


Fig. 3.6.4.6 **Initial and final model configurations for NCAP test (35 mph)**

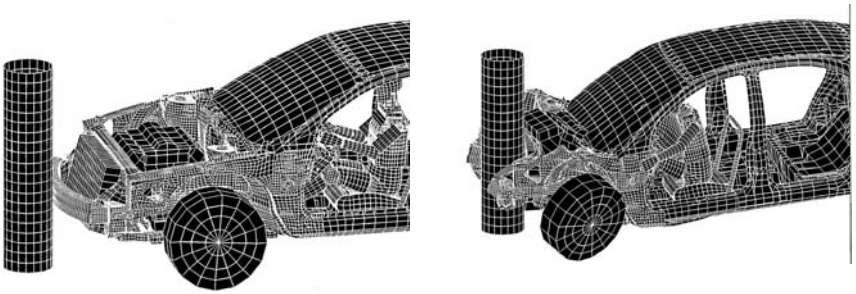


Fig. 3.6.4.7 **Initial and final model configurations for pole impact test (30 mph)**

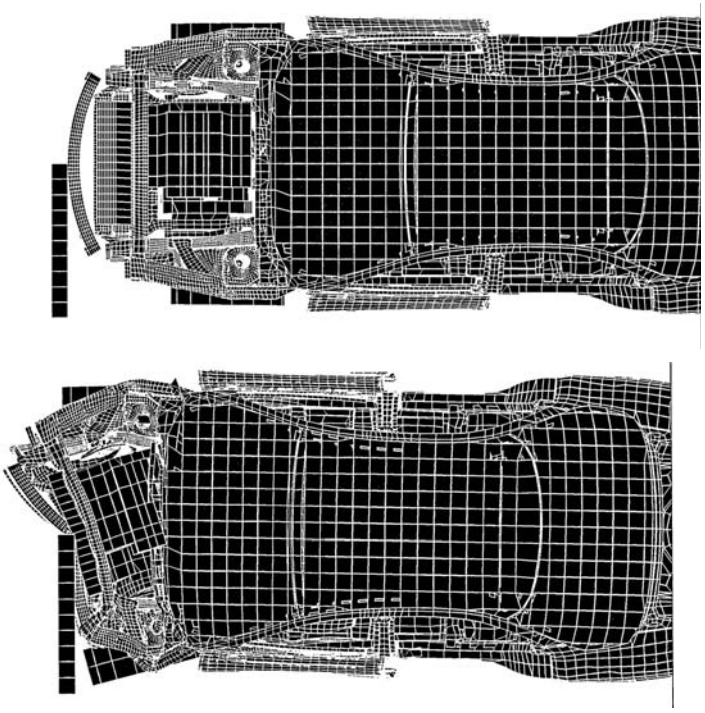


Fig. 3.6.4.8 **Initial and final model configurations for offset test 30 mph)**

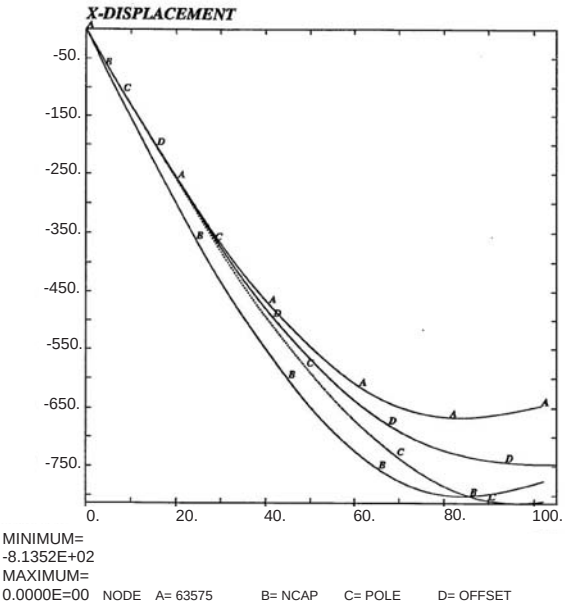


Fig. 3.6.4.9 **Frontal vehicle deformations for 30 mph, NCAP**

frontal, side, rear vehicle impact with barriers. Vehicle-to-vehicle collisions were also developed and analyzed. In addition to vehicle structural modeling, dummy and air bag models were created and their responses were validated against experimental data.

In 1995 [51], a process was established to integrate vehicle structure, instrument panel, steering assembly, driver air bag and Hybrid III dummy models in a single FE model. This process centered on integrating existing components and subsystem models and clearly demonstrated that explicit FE technology can simulate both structural and restrained occupant response resulting from a vehicle crash in a single integrated model, although the results are preliminary.

3.8 References

1. Rapin, M.P., (1970) Vehicle Structural Crashworthiness in Proceedings of 1970 International Automobile Safety Conference Compendium, Detroit, Michigan, pp. 927-940.

2. Kamal, M.M. (1970) Analysis and Simulation of vehicle to Barrier Impact, *Society of Automotive Engineers*, SAE Paper No. 700414.

3. Wang, H.C. and Merdith, D., (1983) The Crush Analysis of Vehicle Structures, International Journal of Impact Engineering, Vol. 1, No. 3, pp. 199-225.

4. Chang, D.C. (1977) A Design-Analysis Method for the Front Crush Strength of Body Structures, SAE Paper No. 770593.

5. McIvor, I.K. (1973) Modeling and Simulation as Applied to Vehicle Structures and Exteriors, Proceedings of Vehicle Safety Research Integration Symposium, DOT HS-820-306.

6. Mahmood H.F. and Paluzeny A. (1986) Analytical Technique for Simulating Crash Response of Vehicle Structures Composed of Beam Elements, *6th International Conference on Vehicle Structural Mechanics*, SAE Publisher.

7. Gamon, M.A., (1978) General Aviation Airplane Structural Crashworthiness User's Manual, Vol.1, Program KRASH Theory, FAA Report No. FAA-RD 77-18.

8. Pifko, A.B. and Winter, R. (1981) Theory and Applications of Finite Element Analysis to Structural Crash, in *Structural and Nonlinear Solid Mechanics*, A.K. Noor and H.G. McComb (eds.), Pergamon Press, Oxford.

9. Argyris, J., Balmer, H.A., ST. Doltsinis, J. and Kruz, A. (1986) Computer Simulation of Crash Phenomena, Int. J. for Numerical Methods in Engineering, 22, pp. 497-519.

10. Ni, C.M. (1981) A General Purpose Technique for Nonlinear Dynamic Response of Integrated Structures, 4th International Conference on Vehicle Structural Mechanics, SAE Publisher.

11. Haug, E., Arnadeau, F., Dubois, J. and De Rouvray A. (1983) Static and Dynamic Finite Element Analysis of Structural Crashworthiness in the Automotive and Aerospace Industries, in *Structural Crashworthiness*, N. Jones and T. Wierzbicki (eds.), Butterworths Publisher, pp. 175-218.

12. Belytschko, T.B. and Hsieh, B.J. (1974) Nonlinear Transient Analysis of Shells and Solids of Revolutio by Convected Elements, *AIAA Journal*, 12, pp. 1031-1039.

13. Winter, R., Mantus, M. and Pifko A.B. (1981) Finite Element Crash Analysis of a Rear Engine Automobile, 4th International Conference on Vehicle Structural Mechanics, SAE Publisher, pp. 55- 61.

14. Haug, E., Scharnhorst, DuBois, P. (1986) FEM-Crash: Berechnung eines Fahrzeugfrontalaufpralls VDI-Tagung, Wuerzburg.

15. Bretz, Jarzab, Raasch, (1986) Berechnung eines Frontalen Crashvorganges bei einer heckangetriebenen Limousine, VDI-Tagung, Wuerzburg.

16. Hieronimus, Nalepa, (1986) Introduction and Use of a Supercomputer at Opel, e.g. for Crash Simulation, International Conference on Supercomputer Applications in the Automotive Industry, Zurich.

17. Gonard, Germain-Lacour, Azais, (1986) International Conference on Supercomputer Applications in the Automotive Industry, Zurich.

18. Isuzu Motors Limited, (1987) Crash Analysis of 760 Coupe, Body Engineering Department, Personal Communication.

19. Benson, D.J. and Hallquist, J.O. (1986) The Application of DYNA3D in Large Scale Crashworthiness Calculations, Lawrence Livermore National Laboratory, *Report No. UCRL*-94028.

20. Nilsson, L. (1989) Computational Crash Analysis at the Saab Car Division, *12th International Technical Conference on Experimental Safety Vehicles*, Goteborg, Sweden.

21. Haug, E., Scharnhorst, T. and Du Bois, P. (1986) FEM-Crash Simulation of a Frontal Impact (VW-POLO), Translated From German, VDI Report 613, pp. 479-505.

22. Bertz, G., Jarzab, W. and Raasch, I. (1986) Computation of a Frontal Impact of a Rear Wheel Drive Car, Translated From German, *VDI Report* 613, pp. 507-525.

23. Scharnhorst, T. I., Rassch, I. and E. Schelke, E. (1986) Conclusiveness of Math Methods for Crash Behavior Simulation of Cars, Translated from German, *VDI Report,* 613.

24. Chedmail, J.F., et al, (1986) Numerical Techniques, Experimental Validation and Industrial Applications of Structural Impact and Crashworthiness Analysis with Supercomputers for the Automotive Industry, International Conference on Supercomputing, Zurich, Switzerland.

25. Nalepa, E. (1989) Crashworthiness Simulation of the Opel Vectra Using the Explicit FE Method, International. Journal of Vehicle Design, IAVD Congress on Vehicle Design and Components, pp. 191-201.

26. Khalil, T.B. and Lin, T.C. (1994) Simulation of the Hybrid III Dummy Response to Impact by Nonlinear Finite Element Analysis, in Proceedings of 38th. Stapp Car Crash Conference, SAE Publisher, pp. 325-345.

27. Zouk, A.K., Marzougui, D. and Bedewi, N. E. (1998) Development of a detailed Vehicle Finite Element Model Part I: Methodolgy, International Crashworthiness Conference, Dearborn, Michigan, Woodhead Publishing Limited, pp. 184-195.

28. Cofie, E. (1994) Finite Element Model of a small Automobile Impacting a Rigid Pole, Office of Safety and Traffic Operations Research and Development, Federal Highway Administration, Final Report, Contract No. NHI GFR Project # 93-31.

29. Newmark, N.M. (1959) A Method of Computation for Structural Dynamics, *J.* Engineering Mechanics Division, ASCE, 67, 67-94.

30. Farhoomand, I. (1972) Nonlinear Dynamic Stress Analysis of Two-dimensional Solids, *Ph.D. Thesis*, University of California, Berkeley, Graduate Division.

31. Hughes, T.J.R., Pister, K.S., and Taylor, R.L. (1979) Implicit-Explicit Finite Elements in Nonlinear Transient Analysis, Computer Methods in Applied Mechanics and Engineering, 17/18, 159.

32. Belytschko, T.B, and Tsay, C.S. (1981) Explicit Algorithms for Nonlinear Dynamics of Shells, AMD, Vol.48, ASME, pp. 209-231.

33. Belytschko, T.B., Lin, J.I., and Tsay, C.S., (1984) Explicit Algorithm for the Nonlinear Dynamics of Shells, Comp. Methods. in Applied Mechanics and Engineering, Vol. 43, pp. 251-276.

34. Belytschko, T.B. Stolarski, H., and Carpenter, N., (1984) A Triangular Plate Element with One-Point Quadrature, International J. of Numerical Methods in Engineering, Vol. 20, pp. 787-802.

35. Flanagan, D.P., and Belytschko, T., (1981) A Uniform Strain Hexahedron and Quadrilateral and Orthogonal Hourglass Control, International Journal of Numerical Methods in Engineering, Vol. 17, pp. 679-706.

36. Belytschko, T.B., and Tsay, C.S. (1983) A Stabilization Procedure for the Quadrilateral Plate Element with One-Point Quadrature, International Journal of Numerical Methods in Engineering, Vol. 19, pp. 405-419.

37. Hughes, T.J.R. and Liu, Y.K., (1981) Nonlinear Finite Element Analysis of Shells: Part II Two Dimensional Shells, Computer Methods in Applied Mechanics, Vol. 27, pp. 331-362.

38. Hughes, T.J.R. and Liu, Y.K., (1981) Nonlinear Finite Element Analysis of Shells: Part I Three Dimensional Shells, Computer Methods in Applied Mechanics, Vol. 27, pp. 167-181.

39. Belytschko, T.B., Wong, B.L., and Chiang, H.Y., (1992) Advances in one-point Quaderature Shell Elements, Computer Methods in Applied Mechanics and Engineering.

40. Sheh, M.Y. and Khalil, T.B. (1991) The Impact Response of a Vehicle Structural Rail by Experiments and Finite Element Analysis in *Symposium on Crashworthiness and Occupant Protection in Transportation Systems,* T.B. Khalil, H.F. Mahmood, C.M. Ni and A.I. King (eds.), ASME Publication, AMD-Vol. 126/BED-Vol. 19, pp. 195-207.

41. Khalil, T.B. and Vander Lugt, D.A. (1989) Identification of Vehicle Front Structure Crashworthiness by Experiments and Finite Element in Symposium on Crashworthiness and Occupant Protection in Transportation Systems, T.B. Khalil, and A.I. King, (eds.), ASME Publisher, AMD-Vol. 106 and BED-Vol. 13, pp. 41-53.

42. Bertz, G., Jarzab W. and Raasch I. (1986) Computation of a Frontal Impact of a Rear Wheel Drive Car, Translated From German, VDI Report ,613, pp. 507-525.

43. Scharnhorst, T. I. Rassch, I. and Schelke, E. (1986) Conclusivness of Math Methods for Crash Behavior Simulation of Cars, Translated from German, VDI Report, 613.

44. Vander Lugt, D.A. et. al. (1987) Passenger Car Frontal Barrier Simulation Using Nonlinear Finite Element Method, SAE Passenger Car Meeting and Exposition, Dearborn, Michigan, Paper No. 871958.

45. Kurimoto, K. et.al. (1989) Simulation of Crashworthiness and its Application, 12th. International Technical Conference on Experimental Safety Vehicles, Goteborg, Sweden.

46. Futamata, T. et. al. 1989) Crash Simulation Methods for Vehicle Development at Nissan, 12th International Technical Conference on Experimental Safety Vehicles, Goteborg, Sweden.

47. Johnson, J.P. and Skynar, M.J. (1989) Automotive Crash Analysis Using the Explicit Integration Finite Element Method, in *Proceedings of Crashworthiness and Occupant Protection in Transportation Systems*, T.B. Khalil, and A.I. King, (eds.), ASME Publisher, AMD-Vol. 106 and BED-Vol. 13, pp. 27-33.

48. Sheh, M.Y. et. al. (1992) Vehicle Crashworthiness Analysis Using Numerical Methods and Experiments, 8th International Conference on Vehicle Structural Mechanics and CAE, Traverse City, Michigan, SAE Publisher, pp. 119-128.

49. Kohlhoff, St et.al. (1994) A Computational Approach to an Investigation of Frontal Car-To-Car Collision for the Development of Barrier Test, Numerical Analysis in Automobile Engineering, VDI Conference Wurzburg, Germany, pp. 467-484.

50. Cheng, J.C. and Doong, J. (1994) Numerical Analysis of Vehicle Crashworthiness in Various Configurations*, Cray Channels,* Vol. 16, No. 2, pp. 8-11

51. Khalil, T.B. and Sheh, M.Y. (1997) Vehicle Crashworthiness and Occupant Protection in Frontal Impact by FE Analysis – An Integrated Approach, in *Proceedings of Crashworthiness of Transportation Systems: Impact and Occupant Protection, Kluwer Academic Publisher, pp. 363-399.*

52. Steyer, C., Diet, S. and Du Bois, P. (1989) Numerical Simulation of the Proposed Side Impact Procedure, in *Proceedings of Crashworthiness and Occupant Protection in Transportation Systems*, AMD-Vol. 106 and BED-Vol. 13, T.B. Khalil, and A.I. King, (eds.), ASME Publisher, pp 53-95.

53. Kaiser, A. (1992) Some Examples on Numerical Simulation in Vehicle Safety Development, 8th International Conference on Vehicle Structural Mechanics and CAE, Traverse City, Michigan, SAE Publisher, pp. 119-128.

54. Calso, S.M. et. al. (1993) Simulation of Offset and In-line car to Car Rear Impact", in *Proceedings of Crashworthiness and Occupant Protection in Transportation Systems*, AMD-Vol. 169 and BED-Vol. 25, J. Reid, and K. Yang (eds.), ASME Publication, pp. 149-161.

55. *PAM-CVS User's Manual*, Version 1.0 (1990), Engineering Systems International, Paris, France.

56. Khalil, T.B. and Lin, K.H. (1991) Hybrid III Thoracic Impact on Self-Aligning Steering Wheel by Finite Element Analysis and Mini-Sled Experiments, in *Proceedings of 35th Stapp Car Crash Conference,* SAE Publisher, pp. 73-85.

57. Ove Arup & Partners International, (1992) An Integrated Approach To Vehicle Crashworthiness and Occupant Protection, Report, Issue 1, London, England.

58. Schelkle, E. and Remensperger, R. (1991) Integrated Occupant-Car Crash Simulation with the Finite Element Method: The Porsche Hybrid III-Dummy and Airbag Model, in Frontal Crash Safety Technologies for the 90's, SAE paper No. 910654.